

## LIA-2 AND BIM ACCELERATORS AS PART OF RADIOGRAPHIC COMPLEX AT RFNC-VNIITF

A. Akhmetov, S. Khrenkov, P. Kolesnikov, E. Kovalev, O. Nikitin, D. Smirnov, Russian Federal Nuclear Center — Zababakhin All-Russian Scientific Research Institute of Technical Physics (RFNC-VNIITF), Snezhinsk, Russian Federation

### Abstract

The paper describes installations included in the radiographic complex at RFNC-VNIITF, their purpose, composition, and principle of operation. The paper presents the synchronizing system for the betatron complex based on BIM pulse air-cored betatrons and LIA-2 linear induction accelerator, as well as the synchronizing circuit and functioning algorithm in the mode of BIM and LIA-2 combined operation. This combined mode of operation was tested and results of this testing are also provided.

### COMPOSITION OF THE RADIOGRAPHIC COMPLEX

The radiographic complex includes the betatron complex consisting of two pulse air-cored betatrons BIM (further – betatron complex) and linear induction accelerator LIA-2 (further – LIA-2). The betatron complex ensures two-direction recording of dynamic objects at 90° between directions. Each betatron in the betatron complex can generate from one to three radiation pulses in one gas-dynamic experiment. LIA-2 is placed between betatrons and can generate up to two radiation pulses.

The betatron complex and LIA-2 are independent units.

The betatron complex is intended study high-speed processes in gas-dynamic experiments using the pulse shadow X-ray diffraction technique. Main technical characteristics of the betatron complex are given in table 1 [1].

Table 1: Main technical characteristics of the betatron complex

Parameter (Units)	Value
Boundary energy of bremsstrahlung spectrum (MeV)	65
Penetrability in Pb (mm)	165
Radiation source size (mm)	2.5x6
Duration of $\gamma$ -radiation pulse in the mode of one radiation peak generation (ns)	100
Max. number of successive pulses	3
Time interval between $\gamma$ -radiation pulses in the mode of three radiation peaks generation ( $\mu$ s)	0.5-5

Penetrability of the betatron complex was estimated based on a X-ray diffraction image of a lead test object "wedge" [2] positioned at the 4-m distance from a target. Maximum thickness of the test object was 100 mm with

the 10-mm step. Two more lead blocks with the total thickness of 100 mm were placed in front of the test object. The recording unit was immediately adjacent to the "wedge". The maximum penetrability of the betatron complex was 180 mm. The X-ray diffraction image of the "wedge" is given in Fig. 1.

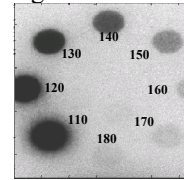


Figure 1: X-ray diffraction image of test object "wedge".

The radiation source size was estimated based on the X-ray diffraction image given by the pinhole camera positioned at the distance of 1 m from the target. The recording unit was positioned at the 3-m distance. The radiation source size was measured at 0.5 blackening density minus background. Blackening density distribution after X-raying of the pinhole camera is given in Fig. 2.

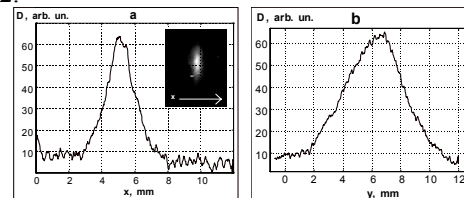


Figure 2: Blackening density distribution after X-raying of the pinhole camera.

Electrons are deflected onto the target either in one pulse or in portions with the formation of up to three X-ray pulses with a certain intensity relation between them depending on a particular task. For this purpose, installation is equipped with generators that deflect the electron beam onto the target. Usually, total energy is distributed as follows: 1-st pulse takes 10-15%, 2-nd pulse – 30%-40%, and 3-d pulse – 50%-60%.

LIA-2 is a high-quality injector of a large-scale linear induction accelerator LIA-20 intended for small-direction X-ray tomography complex. Thanks to high-quality of the formed electron beam, LIA-2 is used as an independent X-ray installation. Main technical characteristics LIA-2 are given in table 2 [3].

Table 2: Main technical characteristics of LIA-2

Parameter (Units)	Value
Max. beam energy (MeV)	2.0
Max. beam current (kA)	2.0

Min. beam spot size on the target in all modes (mm)	1.5
Current pulse length (ns)	180
Max. number of successive pulses	2
Time interval between pulses (μs)	3-20

LIA-2 penetrability is determined with the help of the test lead “wedge” positioned at the distance of 1.5 m from the target. Maximum thickness of the “wedge” was 100 mm.

Fig. 3 shows the X-ray diffraction image of the lead “wedge” with the electron energy of 1.1 MeV. LIA-2 penetrability at the observability limit is 60 mm in lead when Image Plate is used for recording.

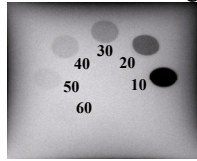


Figure 3: Penetrability determination at 1.1MeV electron energy.

Fig. 4 shows the X-ray diffraction image of the lead “wedge” with the electron energy of 1.3 MeV. With this electron energy, LIA-2 penetrability equals 70 mm.

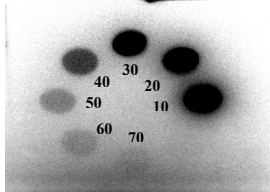


Figure 4: Penetrability determination at 1.3MeV electron energy.

Fig. 5 shows the X-ray diffraction image of the lead “wedge” with the electron energy of 1.5 MeV. With this electron energy, LIA-2 penetrability equals 70 mm.

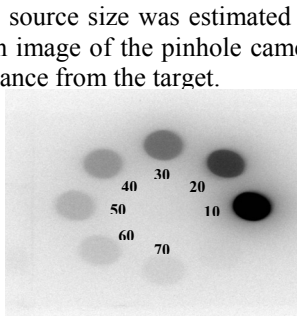


Figure 5: Penetrability determination at 1.5MeV electron energy.

The recording unit was positioned at the 3-m distance. The radiation source size was measured at 0.5 blackening density minus background. Fig. 6 shows X-ray diffraction image of the pinhole camera.



Figure 6: X-ray diffraction image of the pinhole camera.

Blackening density distribution after X-raying of the pinhole camera is given in Fig. 7.

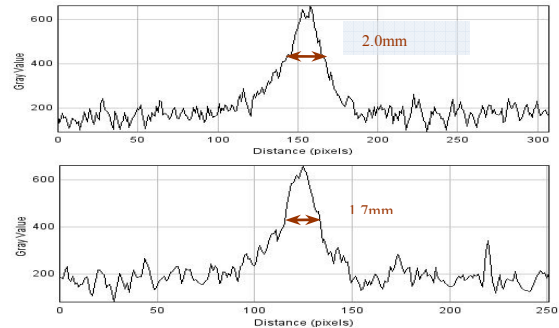


Figure 7: Blackening density distribution over the horizontal and vertical axes, respectively.

### SYNCHRONIZING SYSTEM

Analysis of time diagrams for technological processes in the betatron complex and LIA-2 in the independent operational mode demonstrated that physical implementation of the synchronizing system is possible. Installations are synchronized through “wedging-in” of the LIA-2 start-up into the betatron complex functioning, i.e. after the switch-on and charging stage and before the injection stage and the acceleration cycle. Duration of the technological process in LIA-2 is ~57 ms, duration of the switch-on and charging stage for the betatron complex is 60 seconds, duration of the injection stage and the acceleration cycle is ~0.4 ms.

Synchronization diagram for the betatron complex and LIA-2 is given in Fig. 8 (numbers denote the sequence of signals formation).

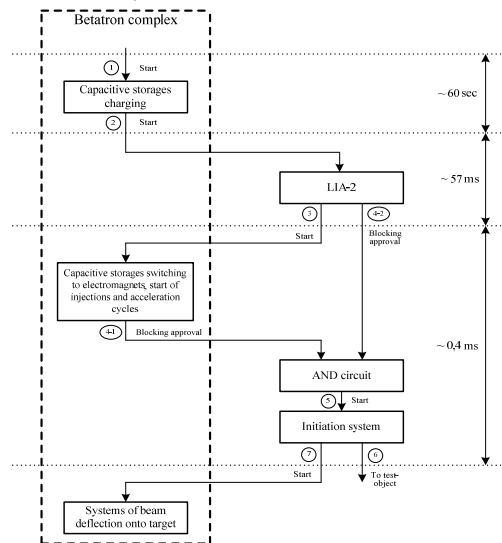


Figure 8: Synchronization diagram for the betatron complex and LIA-2.

Fig. 9 shows the synchronization algorithm block-diagram for the betatron complex and LIA-2 operation.

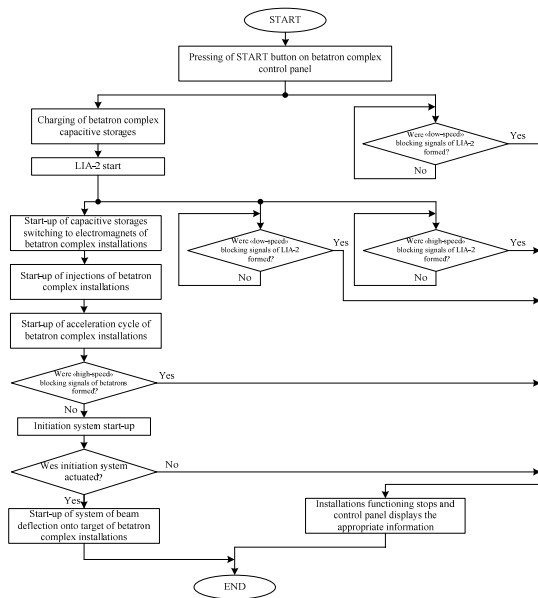


Figure 9: Synchronization algorithm block-diagram for the betatron complex and LIA-2 operation.

Pressing the button START on the control panel of the betatron complex initiates start of the betatron complex and LIA-2 in the mode of combined synchronized operation. Then, all capacitive storages of the betatron complex are charged.

Then, functional parts and systems of LIA-2 are started up; time delays of their start-up are preliminarily adjusted on the LIA-2 control panel [4]. Somewhere about 300-450  $\mu$ s prior to the  $\gamma$ -radiation pulse generation, the LIA-2 control system forms the signal to continue BIM start.

In parallel, operation of all LIA-2 units and systems, as well as of the betatron complex is controlled. In the case of any discrepancies in the technological process, an appropriate blocking signal is formed to stop betatron complex functioning; the control panel displays the appropriate information.

In the normal mode of initiation system actuation, the system of beam deflection onto the target of each installation of the betatron complex is initiated and  $\gamma$ -radiation pulses are generated. Fig. 10 shows the time diagram for the combined synchronized operation of the betatron complex and LIA-2.

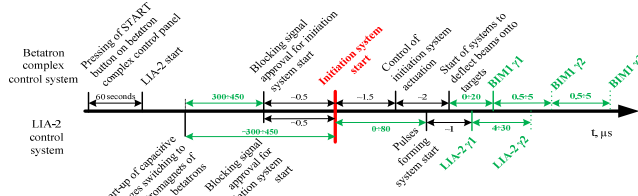


Figure 10: Time diagram for the combined operation of installations.

### TESTING

Testing of the combined mode of betatron complex and LIA-2 operation included a series of start-ups with the

registration of  $\gamma$ -radiation pulses. These tests allowed us to record  $\gamma$ -radiation pulses of the betatron complex and LIA-2. Time delays in the recorded  $\gamma$ -radiation pulses were observed to correspond to those specified. A typical oscilloscope record of  $\gamma$ -radiation pulses recorded during a technological start-up of the betatron complex and LIA-2 in the combined operation mode is given in Fig. 11 where: channel 1 – is the signal of the initiation system start; channels 2 and 3 – are signals of  $\gamma$ -radiation pulses from installations of the betatron complex; channel 4 – are signals of  $\gamma$ -radiation pulses of the betatron complex and LIA-2.

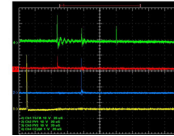


Figure 11: Oscilloscope record of  $\gamma$ -radiation pulses.

### CONCLUSION

Nowadays, the radiographic complex at RFNC-VNIITF includes a number of up-to-date installations that can successfully meet challenges of gas dynamic testing.

By now, the combined operation mode was tested for the betatron complex and LIA-2 with the generation of  $\gamma$ -radiation pulses at a specified instant.

Radiographic installations capable of generating both soft and hard radiation spectra will allow one to solve a wider range of tasks during the same explosive experiment. Combined operation of the betatron complex and LIA-2 will also provide X-ray diffraction images in 3 directions during the same explosive experiment.

Development of appropriate recording systems will allow realization of inherent potential and, on the whole, increase operation efficiency of the radiographic complex at RFNC-VNIITF.

### REFERENCES

- [1] Y Kuropatkin, V Mironenko, V. Tsybrev, A. Kostin, V. Kotilevskiy, "Technical description of the installation BIM for X-ray radiography of high-speed processes," R&D report (intermediate), VNIIEF, 2000.
- [2] Y. Kuropatkin, S. Voronov, V. Suvorov, V. Mironenko, D. Grishin, V. Tsybrev, A. Kostin, V. Kotilevskiy, "Radiographic characteristics of installation BIM to study high-speed processes," R&D report (intermediate), VNIIEF, 2001.
- [3] P. Logachev, A. Batrakov, A. Pavlenko, V. Sazanskiy, G. Fatkin, "Automation system for the linear induction accelerator of the radiographic complex," Vestnik NGU (Reporter of Novosibirsk State University), Novosibirsk, 2010.
- [4] P. Logachev, P. Bak, A. Batrakov, R. Kadyrov, A. Pavlenko, A. Panov, V. Sazanskiy, G. Fatkin, "Control system for the linear induction accelerator of the radiographic complex: structure, hardware, trial operation results," Novosibirsk, 2011.